Available online at www.sciencedirect.com

ScienceDirect

Journal of Taibah University for Science 10 (2016) 412–429

Journal of Taibah University for Science

www.elsevier.com/locate/jtusci

Review Article

Exploitation of $KMnO_4$ material as precursors for the fabrication of manganese oxide nanomaterials

Khalid Abdelazez Mohamed Ahmed [a,b,*]

[a] *Department of Chemistry, Faculty of Science and Technology, Al-Neelain University, P.O. Box 12702, Khartoum, Sudan*
[b] *Department of Chemistry, Faculty of Science and Education, Taif University, P.O. Box 888, 5700, Saudi Arabia*

Received 18 April 2015; received in revised form 15 June 2015; accepted 28 June 2015
Available online 29 August 2015

Abstract

Since the first synthesis of $KMnO_4$ using pyrolusite mineral and potassium carbonate, the experimental synthesis of manganese oxide nanostructures and their application to multiple scientific disciplines have been undertaken extensively. In this review, potassium permanganate raw materials were shown to be more effective and versatile than other addition materials; therefore, they have been widely used to synthesize a variety of manganese oxide nanomaterials, including manganese dioxides, trioxides, tetraoxides, oxyhydroxides and metal-incorporated oxide nanomaterials. Recent progress focused on the synthesis and analysis of the novel characteristics of Mn-oxide nanostructures, emphasizing critical experiments to determine the chemical and physical parameters and the interplay between synthetic conditions and nanoscale morphologies. The Crystal Maker Demo program was applied to estimate the anisotropic transformations from $KMnO_4$ to Mn-oxide nanomaterials.

Keywords: Potassium permanganate; Manganese oxides; Nanostructures; Synthesis

Contents

* Correspondence to: Department of Chemistry, Faculty of Science and Education, Taif University, P.O. Box 888, 5700, Saudi Arabia. Tel.: +966 552639984.
E-mail address: khalidgnad@hotmail.com
Peer review under responsibility of Taibah University.

Production and hosting by Elsevier

http://dx.doi.org/10.1016/j.jtusci.2015.06.005

1. Introduction

Transition metal oxides are important for the development of new materials with functionality and intelligence. In particular, because of their unique material properties, transition metal oxide nanomaterials and their assemblies have been widely used in various fundamental research and technological applications [1–4]. The size- and shape-dependent properties of the metal oxides with tailored morphologies and patterns encouraged scientists to prepare metal oxide nanostructures with a controlled size and structure. It is desirable for the preparation of metal oxides to proceed through a simple, effective and inexpensive technique [5,6]. The performance of this material depends on its properties, thus relying on the atomic structure, composition, microstructure, defects and interfaces [7–9]. The preparation procedures for metal oxide nanocrystals, however, showed diverse results. Using a reduction method is one of the common routes to create metal oxide nanocrystals. Among the routes, chemical methods have been proven more effective for preparing various nanocrystals [10,11].

Since its discovery in 1659, potassium permanganate has a long history of application to different fields, such as catalysis, medicine and electrochemical and mechanical areas [12]. It is used as an oxidant in drinking water, wastewater and industrial processes [13–28]. The use of potassium permanganate in the synthesis area was achieved to prepare many manganese oxide nanostructures [29–41]. In addition, potassium permanganate has been used as an astringent in medical applications and as a cathode electron acceptor for microbial fuel cells, which could recover much more electrical power compared with using other existing types of electron acceptors. Thus, the electrochemical regeneration process was investigated on a platinum electrode for the oxidation of quinoxaline and the generation of pyrazine-2,3-dicarboxylic acid [42–48].

Over the last few years, the chemical solution routes have emerged as effective, convenient, and energy-efficient material synthetic techniques for the preparation of nanomaterials. Due to its economy and high degree of compositional control, the hydrothermal method is a preferred route for manganese oxide nanomaterial fabrication.

The aim of this article is the following: (1) to provide a brief account of the utilization of potassium permanganate to generate various types of manganese oxide nanomaterials; (2) to investigate the characterizations of shape, chemical composition and nanostructure through the CMDT program; (3) to address experimental issues related to growth mechanisms to discover new methods for better control; and (4) to note the potential effects of manganese oxide nanostructures on physiochemical applications.

2. Progress of potassium permanganate

2.1. Crystal structure

Potassium permanganate exhibits a wealth of physical and chemical properties originating from the electronic states of Mn^{7+} ($3d^0$) tetrahedrally surrounded by four oxygen anions. However, a study of the $KMnO_4$ crystal before manganese oxide nanocrystal synthesis has not been performed. In Fig. 1(a), four types of $KMnO_4$ crystals were investigated using X-ray diffraction (XRD) patterns. The diffraction peaks of the crystals are exclusively indexed to an orthorhombic unit cell with a space group of Pnma 062, according to standard data JCPDS card Nos. 01-725, 07-023, 44-268 and 73-458 [49]. Therefore, all of the materials have different lattice parameters and Miller indexes in the same crystal phases. The symmetries of the $KMnO_4$ crystals are $2Di\text{-}16\,(V_h^{16})$, and the structure may be given by the following parameters, expressed as fractions of the unit cell dimensions: four K at 4*c*: $u = 0.06$, $v = 0.16$; four Mn at 4*c*: $u = 0.18$, $v = 0.67$; four O at 4*c*: $u = 0.00$, $v = 0$; four O at 4*c*: $u = 0.26$, $v = 0.49$; and eight O at 8*d*: $x = 0.19$, $y = 0.22$, $z = 0.80$ [50,51]. The quantum theory of atoms in molecules was applied to characterize the topological parameters at the bond critical points of the density values that were reported by Marabello et al. [52] revealing

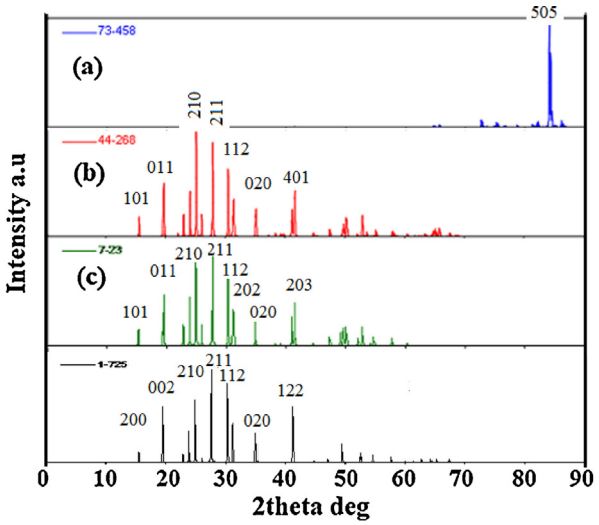

Fig. 1. XRD pattern of potassium permanganate [49].

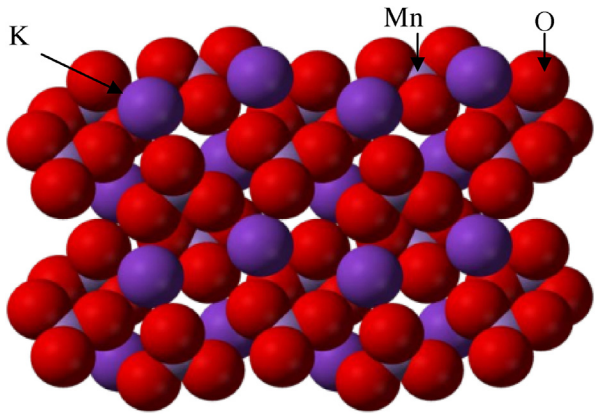

Fig. 2. Crystal structure of potassium permanganate [52].

that the K–O bond has pure ionic characteristics, while the Mn–O bonds show an intermediate behaviour of electron density, which is in good agreement, even on a quantitative level (Fig. 2).

3. Synthesis of Mn-oxide nanomaterials

3.1. MnOOH nanostructures

MnOOH is an important precursor for the synthesis of intercalation compounds, such as lithium manganese oxides, which are potentially inexpensive, environmentally friendly, positive materials for separation-based sensors in biology, electronics and in rechargeable lithium ion batteries. By simply adding inorganic salt, such as ammonium chloride and potassium iodide or N,N-dimethyl ammonium formate (DMF), and ethanol reagents to $KMnO_4$, this one-step process often results in nanorods of γ-MnOOH with specific characteristics, such as low surface area and relatively high uniform phases, similar to the solutions-based synthetic reaction approaches that are seldom used in research [53–56]. As discussed above, the addition of multiple redox materials to $KMnO_4$ results in a one phase structure and an intermediate lamellar structure product, which is supported by the fact that the permanganate ion is important for growing rod structures. The reduction of permanganate by a formaldehyde solution with a slow reaction rate and at a low temperature leads to the formation of MnO(OH) nanorods with a diameter of 50–60 nm and a length of 2–3 μm (Fig. 3(a) and (b)). The reduction, nucleation and growth are accelerated, and octahedron-like microcrystals are obtained. Meanwhile, MnO(OH) must be dehydrated, and a portion is reduced to produce octahedron-like Mn_3O_4 products at a higher temperature (Fig. 3(c) and (d)) [57]. This result suggested that the conversion process from precursor nanorods to an octahedron structure could be rationally expressed by the Ostwald ripening process mechanism. However, oxygen-bonding interactions between the carbonyl function in formaldehyde and the carboxylic acid in formic acid on the permanganate surface were proposed to explain the role of this material in the construction mechanism. Li et al. [58] reported the growth of multiple branched MnOOH nanorods with angles of either 57° or 123° (approximately) that typically contain edge dislocations due to polyethylene glycol and the control of the reaction time (Fig. 4). By comparing this precursor with our previous work, all of the branched nanorods are generally obtained under different reaction conditions, thus limiting the role of additive materials and reaction environments. The synthesis of branched nanostructures has drawn tremendous attention because of their outstanding structural diversity, physical and chemical properties and potential device applications, such as in sensors, optics, energy conversion, electronics, catalysts, and medicine. In all of these cases, the chemical reactions employed for the synthesis of MnOOH nanocrystals can be illustrated as follows (Eqs. (1)–(5)):

$$3KMnO_4 + 4NH_4Cl \rightarrow 3MnOOH + 3KCl + HCl + 6H_2O + 2N_2 \quad (1)$$

$$KMnO_4 + KI + H_2O + ½O_2 \rightarrow MnOOH + KIO_3 + KOH \quad (2)$$

$$KMnO_4 + 2(CH_3)_2NCOH \rightarrow MnOOH + (CH_3)_2NCOOH + (CH_3)_2NCOOK \quad (3)$$

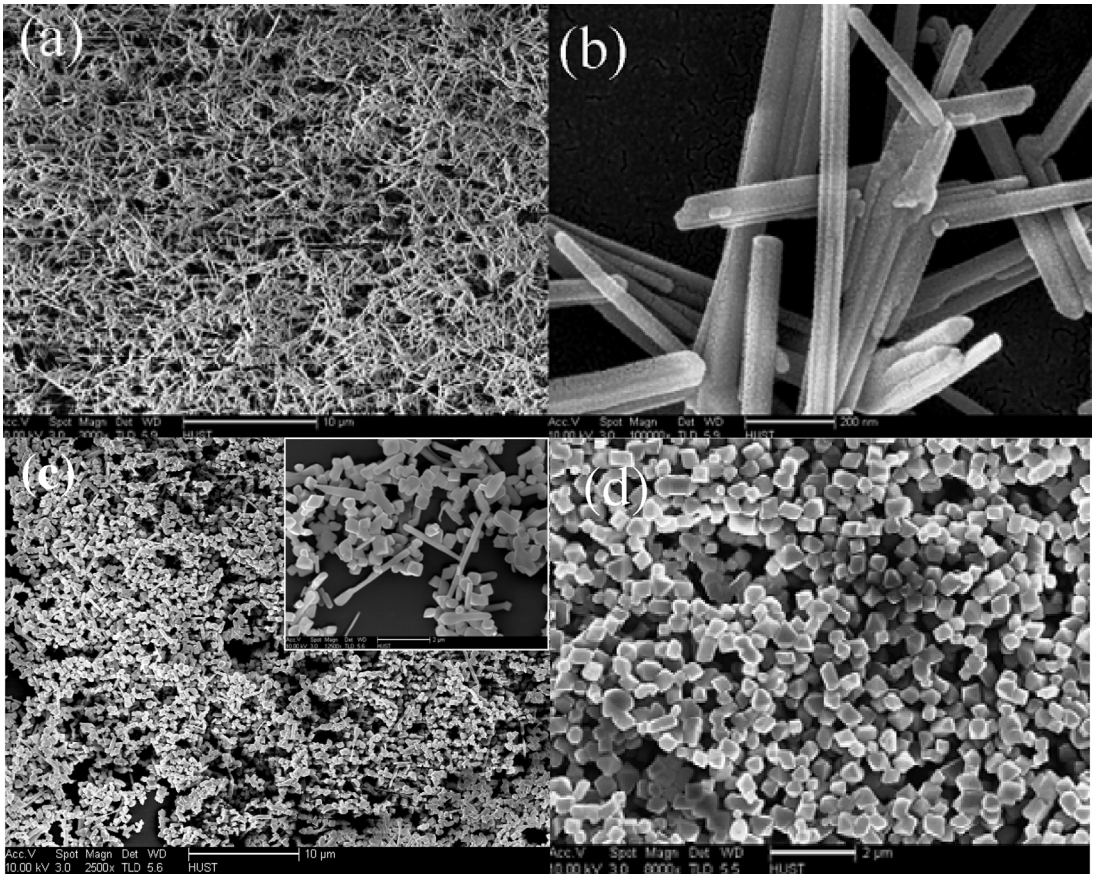

Fig. 3. FE-SEM images of as-synthesized products by the hydrothermal process for 10 h under different temperatures: (a, b) 120 °C, (c) 180 °C and (d) 200 °C [57].

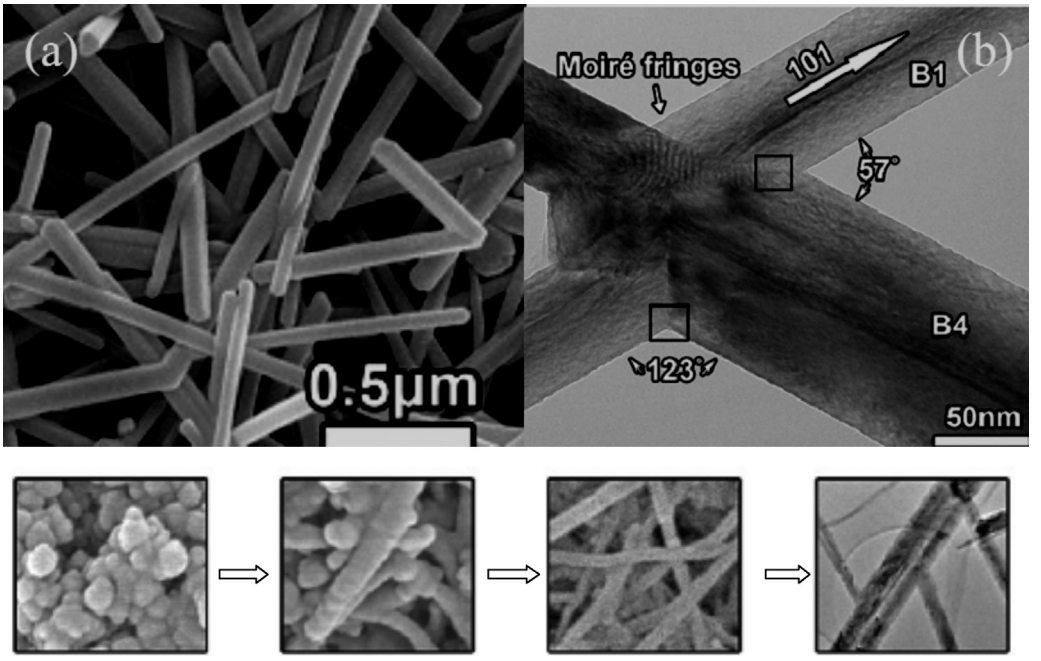

Fig. 4. SEM and TEM images of the as-prepared branched MnOOH nanorods and effect of reaction time and the concentration of the final product [58].

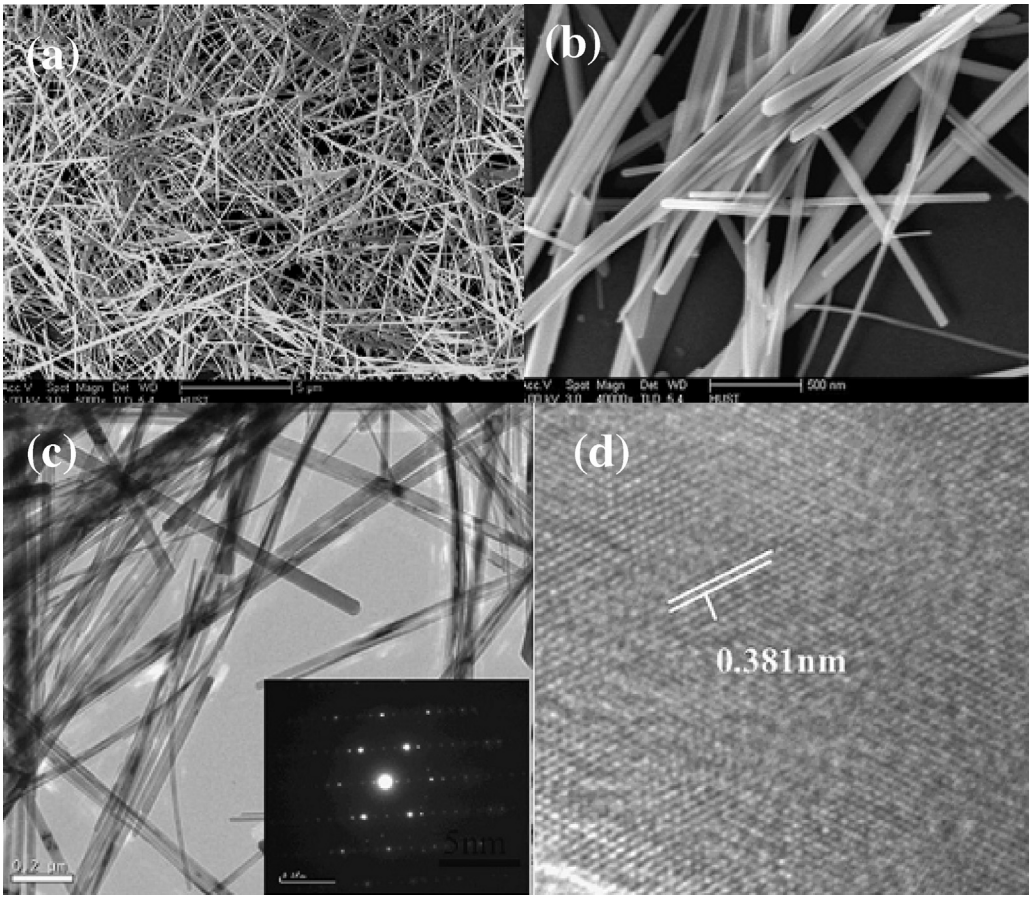

Fig. 5. FE-SEM images of the as-synthesized Mn(OH)O nanowires by hydrothermal reaction between potassium permanganate and ethylene glycol [60].

$$KMnO_4 + 2CH_3CH_2OH \rightarrow MnOOH + 2CH_3CHO + KOH + H_2O \quad (4)$$

$$KMnO_4 + 2CH_2O \rightarrow MnOOH + CHOOH + CHOOK \quad (5)$$

Due to their many low-dimensional characteristics that are different from the bulk properties, MnOOH nanowires have received considerable attention as transistor components, sensing devices, transparent-flexible electronics and memory-integrated logic circuits. In most cases, these γ-MnOOH nanowires were used as catalysts in a rechargeable nonaqueous lithium-oxygen battery to improve the discharge capacity and cycle stability. Due to low production cost, scalability and reduced temperature, the solvothermal synthesis technique is one of the most important methods for the preparation of γ-MnOOH nanowires by the reduction of $KMnO_4$ with polyvinylpyrrolidone [59]. Ethylene glycol is another reducing material to generate Mn(OH)O nanowires with an average diameter of 60–80 in., several tens of micrometres in length, as single crystals and with a space fringe of {2 1 0}, which explained the structural mechanism from the orthorhombic $KMnO_4$ conversion to monoclinic Mn(OH)O due to the oxidation of ethylene glycol to glyoxal (Fig. 5) [60]. Portehault et al. synthesized manganite nanowires, hausmannite nanoparticles and feitknechtite triangular phases using the reduction of permanganate and thiosulfate [61]. He suggested that these evolutions appeared according to a dissolution recrystallization process and the lateral aggregation of primary nanorods.

Xia et al. [62] reported the synthesis of MnOOH nanobelts using a wet chemical method. Fig. 6 shows the nanobelts with a length of several micrometres, a width of 20 mm, fringe spacings in the {2 2 −2} direction, which can be observed using the route from manganese acetate tetrahydrate and $KMnO_4$ in boiling

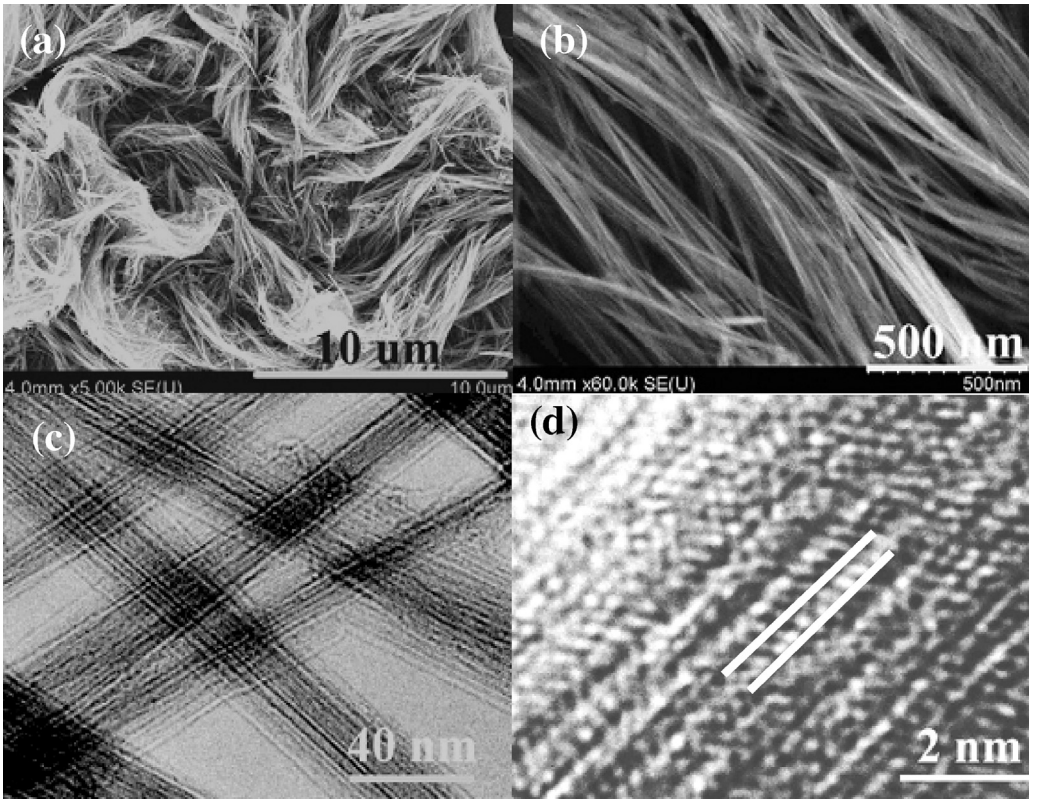

Fig. 6. SEM and HR-TEM images of MnOOH nanobelts prepared by the reflux route utilizing permanganate and pure water at 100 °C for 4 h [62].

water under reflux. The nanobelts exhibited unique electrochemical characteristics for the simultaneous detection of dopamine from ascorbic acid and uric acid when modified with a glassy carbon electrode. From a positive perspective, the synthesis of MnOOH nanostructures not only enabled authors to gain in-depth knowledge of the relationship between the properties, size, shape, and compositions but also enabled use of the nanostructures in a variety of applications in catalysis, ion exchange, separation, molecular sieves and energy storage in secondary batteries [63–67]. To date, only a few reports describe the importance of permanganate in the formation of MnOOH nanocrystals, and most of the research focuses on reducing materials. The precursors of this material are often obtained in many reaction process stages, and the kinetic reactions may be highly complex under the appropriate conditions.

3.2. MnO_2 nanostructures

MnO_2 nanomaterials have attracted increasing interest due to their importance in basic scientific research and their potential technological applications as heterogeneous catalysts for ozone decomposition, for organic pollutants oxidation, nitric oxide detraction, carbon monoxide reduction and degradation of dyes. In addition, these nanomaterials have been used to enhance the performance of lithium-ion batteries [68–77]. Many studies have been performed to investigate MnO_2 nanostructures, such as sonochemical synthesis solution-combustion, thermal decomposition, hydrothermal synthesis, sol–gel, electrodeposition and microwave-assisted synthesis processes [78,79]. Based on $KMnO_4$ as the raw material precursor, many experimental attempts were employed to synthesize MnO_2 nanostructures with different crystallographic forms. Compared with other processes that contain manganese salts, such as chloride, nitrite, carbonate and sulfate, the preparation of α-MnO_2 nanostructures through the permanganate procedure is easy to control and enables different sizes, shapes and functionalities. The reduction of $KMnO_4$ was followed by the use of $K_2Cr_2O_7$ or manganese salts to investigate α-MnO_2 nanorods [80–86]. Some precursor routes require nitric acid and CTAB to precipitate the final products. $MnSO_4$ is used as the reducer to promote the growth of γ-MnO_2 crystallites and to promote the subsequent phase transformation from γ-MnO_2 to α-MnO_2

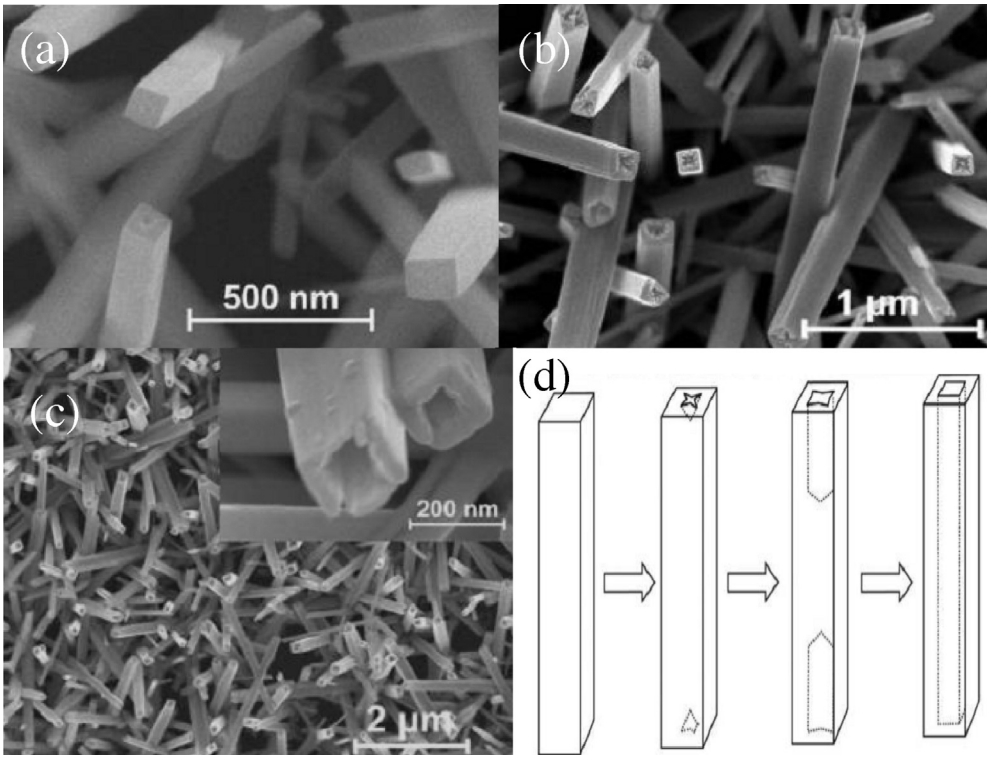

Fig. 7. SEM images of α-MnO_2 nanotubes prepared by a hydrothermal approach employing $KMnO_4$ and HCl at 140 °C for different times: (a) 160 min, (b) 160 min, (c) 12 h and (d) schematic illustration of the etching process [89].

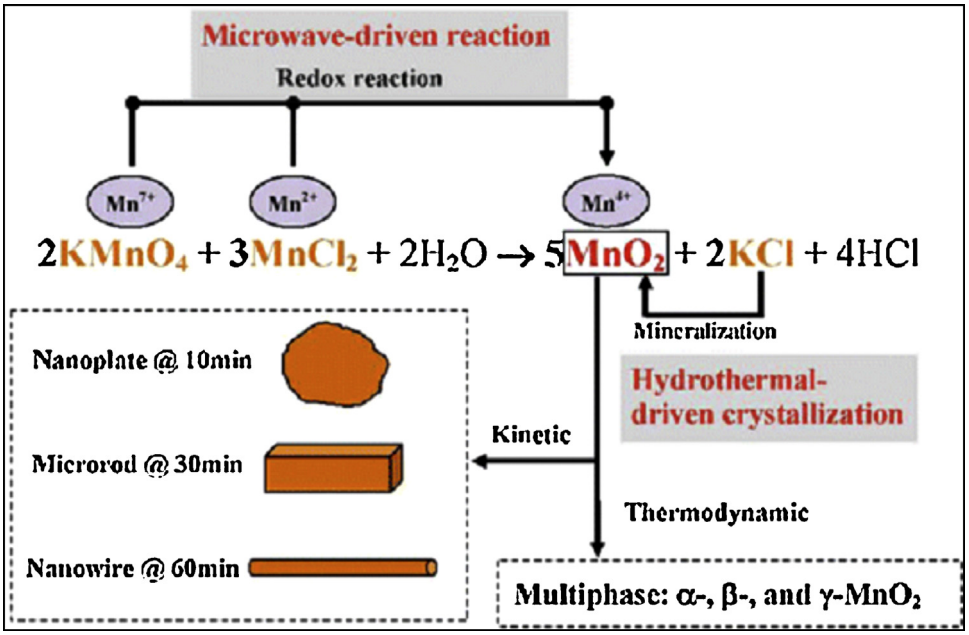

Fig. 8. Schematic illustration of α-, β-, and γ-MnO_2 nanoplates, nanorods, and wire-like shapes via a controllable redox reaction time in the $MnCl_2$–$KMnO_4$ aqueous solution system [90].

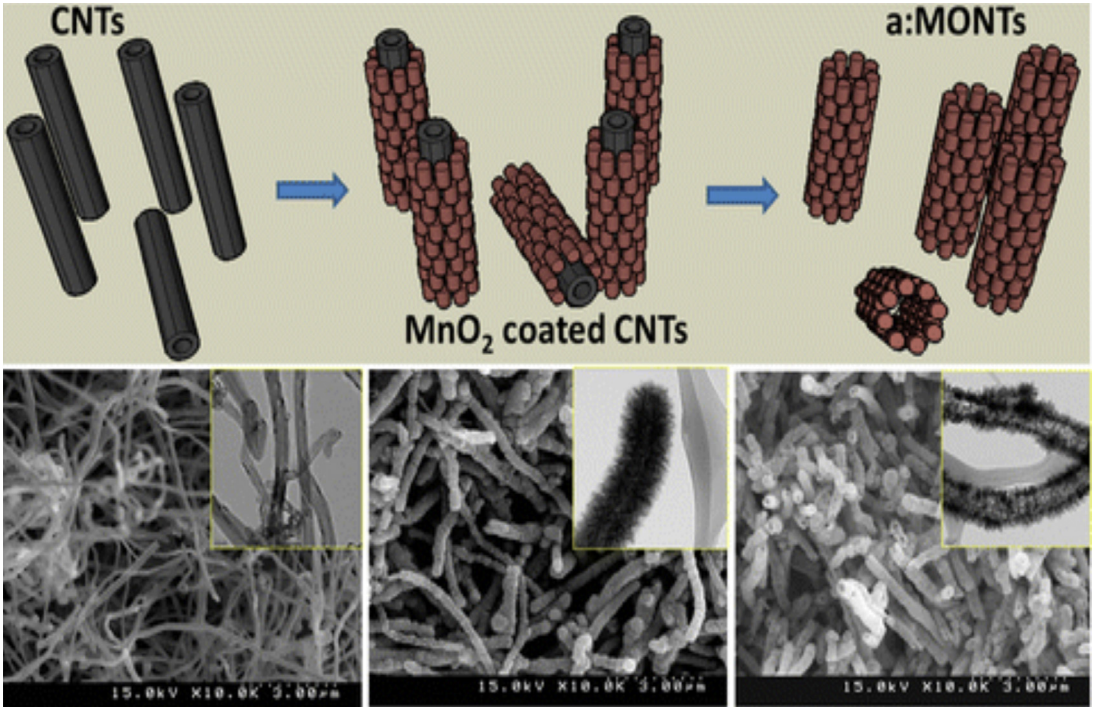

Fig. 9. Schematic investigations of hollow manganese oxide nanotubes on multiwalled carbon nanotubes and in acidic medium [91].

nanorods. The growth mechanism during this process could be attributed to a condensation reaction of the lamellar birnessite structure sheets, leading to a better discharge capacity than the commercial electrolytic manganese dioxide. Acidification of permanganate by sulfuric and hydrochloric acids provided the special phase of urchin with a hollow sphere and nanotube structures [87–89]. Hollow crystals have a very loose mesoporous cluster structure consisting of thin plates or nanowires, and they exhibit enhanced rate capacity and cycleability. The tubular structures occur due to the release of chlorine gas from a solid rod over time (Fig. 7). Chen et al. [90] reported the coupled microwave-hydrothermal process to prepare α-, β-, and γ-MnO_2 with phase structures, such as nanoplate, nanorod and nanowire (Fig. 8). MnO_2 nanocrystals prepared using this method have been applied to electrochemical applications for lithium-ion batteries and for supercapacitors. α-MnO_2 is favourable for the application of supercapacitors due to its tunnel structures. Despite the intercalation–deintercalation reactivity, γ-MnO_2 showed a better anode performance for lithium-ion batteries than other crystal forms. Under heat treatment and acidic medium, the hollow manganese oxide nanotubes with porous walls were also obtained during the release of multiwalled carbon nanotubes (Fig. 9). Typical for this process, the tubular hollow structures were observed after removing the carbon nanotubes, showing a good catalytic performance for the degradation of organic dye under ambient conditions due to the numerous surface reaction sites within the porous hollow tubular structures [91]; potassium ions play an important role in this formation.

Thermal calcination of MnOOH precursors is one of the most common methods to prepare the various MnO_2 nanostructures with unique physicochemical properties. Yang et al. [92] obtained β-MnO_2 nanorods by calcining the γ-MnOOH nanorod precursor, which was prepared from $KMnO_4$ and ethanol. Various manganese oxide nanorods, such as β-MnO_2, Mn_2O_3 and Mn_3O_4, are obtained by the calcination of γ-MnOOH nanorods. α-MnO_2 nanorods appear from the reaction of permanganate and manganese acetate through a redox hydrothermal process without calcinations. In a hydrothermal treatment of only a $KMnO_4$ solution [93], 3D flower-like hierarchical spheres composed of small nanosheets and nanobelts of manganese oxide were reported [94]. Factors such as temperature and Coulomb interaction were proposed to control the formation mechanism. In addition, MnO_2 hierarchical hollow nanostructures occur from the reduction of $KMnO_4$ with $MnCO_3$ in HCl medium [95]. Hybrid/nanocomposite formation of manganese oxide using $KMnO_4$ as the precursor with other materials, such as copper oxide,

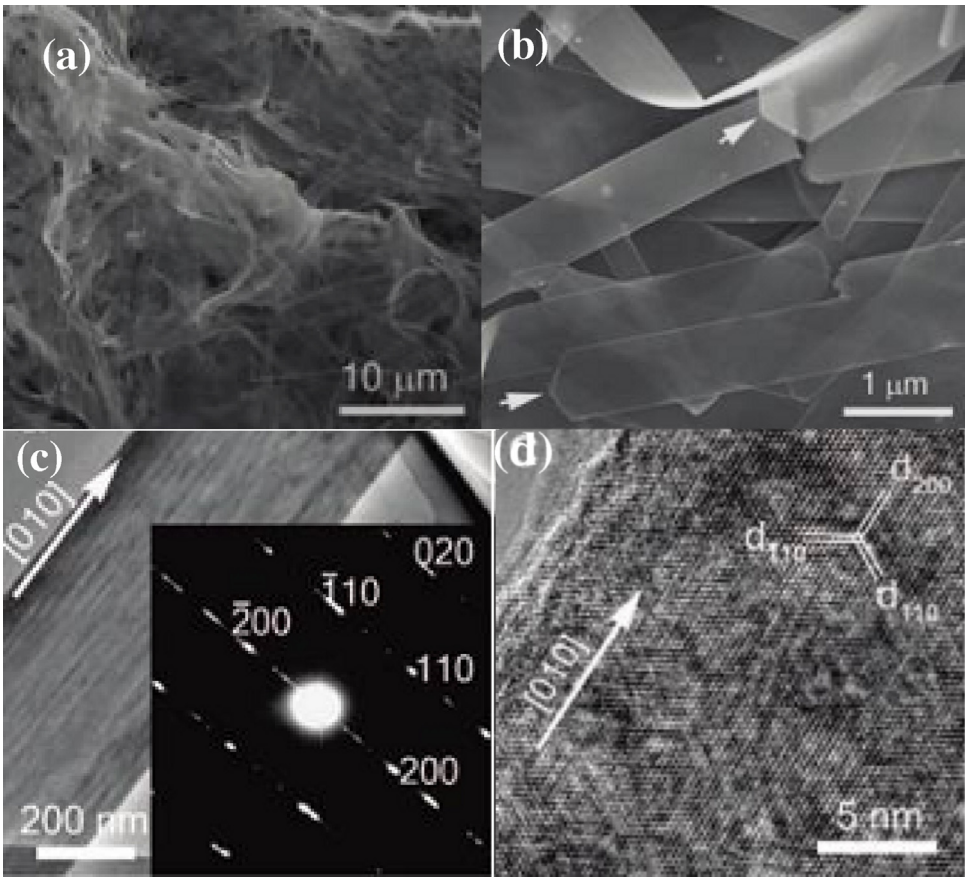

Fig. 10. SEM images of Mn_2O_3 nanospheres, nanocubes, nanoellipsoids, and nanodumbbells prepared by following the $MnCO_3$ and $KMnO_4$ process [106].

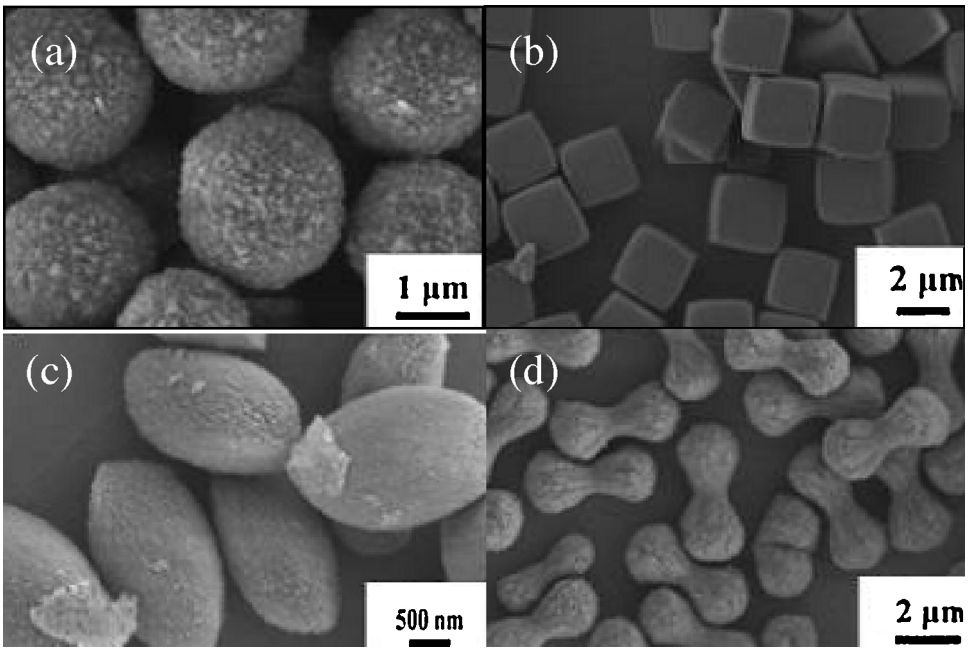

Fig. 11. FE-SEM, TEM and HR-TEM images of the necklace-like Mn_2O_3 nanowire by the calcination route of Mn(OH)O nanowires at 900 °C for 2 h [42].

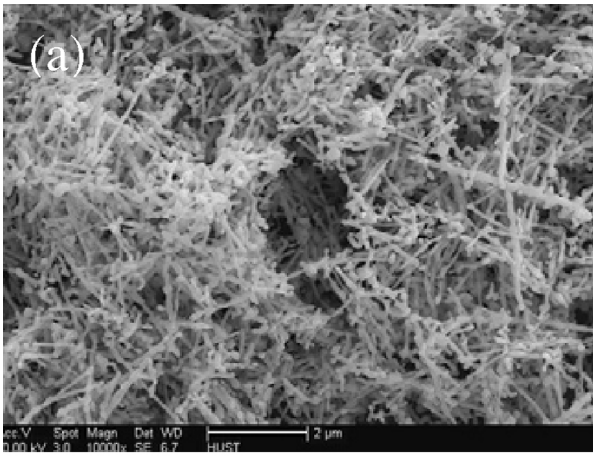

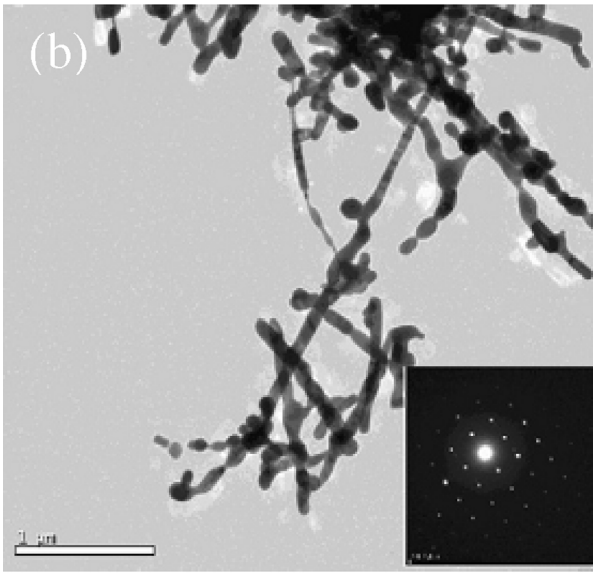

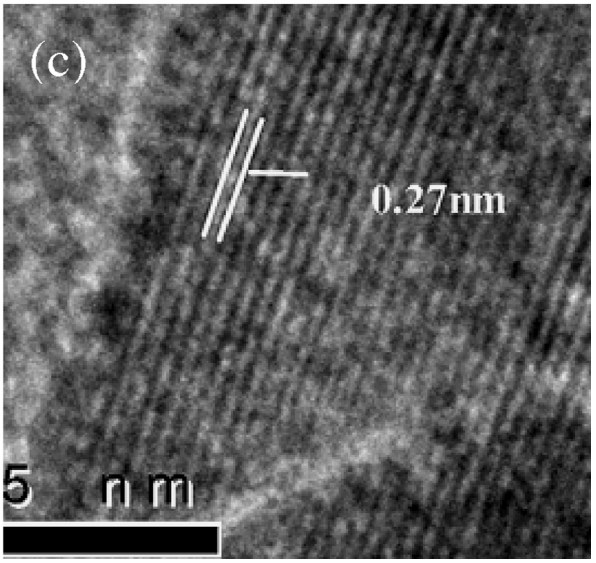

silicon dioxide, iron salts, carbon nanotube, and graphene, can result in interesting nanostructures with improved physicochemical properties. Hollow structures with a star morphology of manganese oxide nanocrystals were obtained by the etching of Cu_2O under template-engaged coordination. The star architecture shows not only a large area but also an ideal capacitive behaviour with a specific capacitance [96]. The hollow structure has also been obtained without assistance from any templates or surfactants through an Fe^{3+} ion and $MnSO_4$ system or by the adduct of SiO_2 spheres and NaOH precursors [17,97]. Porous silica structures with thin catalytic active amorphous MnO_2 nanoparticles were obtained by treating the precursors in bio-silica and acidified permanganate solution [98].

3.3. Mn_2O_3 nanostructures

The synthesis of Mn_2O_3 nanostructures that exhibit better properties for different applications has been investigated over the past years [99–101]. Therefore, the investigations of Mn_2O_3 nanocrystals have become the new focus in the field of materials science and engineering technology [102]. Many synthetic materials of $KMnO_4$ have been explored to introduce Mn_2O_3 nanomaterials. Using hydrazine solutions or tetraethyl ammonium hydroxide under nitric acid or γ-ray radiation conditions at ambient temperatures, γ-Mn_2O_3 nanocrystals were reported [103–105]. Fig. 10 shows the hollow structures of Mn_2O_3 with various phases, such as spheres, cubes, dumbbells, microcubes, microellipsoids and microspheres, that were constructed after a process using permanganate with manganese carbonate [106,107]. Fig. 11 presents the bixbyite-C Mn_2O_3 nanowires after thermal dehydration of Mn(OH)O nanowires. TEM and HR-TEM images reveal that the single crystal grows preferentially along the {2 2 2} direction from the opposite direction of Mn(OH)O, according to the {0 1 1} plane of $KMnO_4$ [42]. Through the intermediate compound of the hollandite-type $K_{1.33}Mn_8O_{16}$ structure and the interaction of $KMnO_4$ with CTAB, 1D-Mn_2O_3 nanorods can be formed [108]. The formation of nanorods using a thermal precursor not only avoids complicated processes and special instruments but also clearly shows the relationship between the structures of the target products and the precursor and is more appropriate for phase control of the morphology. Dang suggested that the role of

Fig. 12. SEM, TEM and HR-TEM images of the as-prepared Mn_3O_4 nanoframes and nanohollows using a polyethylene glycol template-assisted route under hydrothermal conditions [119].

potassium ions is crucial for the crystalline manganese oxide formation. Potassium ions are believed to act as a template for the formation of Mn_2O_3 nanorods, and the conversion efficiency increases with the increasing content of potassium [109].

3.4. Mn_3O_4 nanostructures

Mn_3O_4 is often synthesized using high-temperature calcinations of either higher manganese oxides (MnO_2, Mn_5O_8, and Mn_2O_3), or Mn^{II} and Mn^{III} oxysalts, hydroxides or hydroxyl oxides [110–114]. Due to their unique size- and shape-dependent properties and their potential applications in magnets, electrodes and catalysis, the controlled synthesis of Mn_3O_4 nanostructures has attracted considerable attention in recent decades The most popular strategies used for the synthesis of Mn_3O_4 nanocrystals is the direct chemical reduction of $KMnO_4$ in the presence of other reducer reagents, such as CTAB, ethanol, methanol, n-hexane, oleylamine, hydrazine, sodium dodecylsulfate, ascorbic acid and metallic salt [115,116]. Mn_3O_4 nanorods are obtained on graphene sheets by a template-free hydrothermal reaction in the presence of ethylene glycol [117]. Based on sodium carboxylmethyl cellulose orthedodecyl-amine-Na_2SO_3-ethanol-dedecylamine-ethanol, formamide or polyethylene glycol, 3D-Mn_3O_4 octahedral structures were obtained via a wet solution template-assisted route [118]. Through a template-assisted hydrothermal route, the distinctive characteristics of Mn_3O_4 nanoframes and hollow octahedral structures were obtained using polyethylene glycol. Accordingly, the microscopic images in Fig. 12 show that the hollow dimension sizes, the single-crystalline phase and the lattice fringes of the tetragonal phase of Mn_3O_4 were achieved via $KMnO_4$ reduction [119]. According to the general approaches to Mn-oxide nanostructures, there is evidence that potassium permanganate as a raw material is likely to have prepared Mn-oxides with novel nanostructures. Fig. 14 shows the anisotropic structures of $KMnO_4$ and as-prepared Mn-oxide crystals through CMDT. The reduction of $KMnO_4$ is strongly deduced by covalent

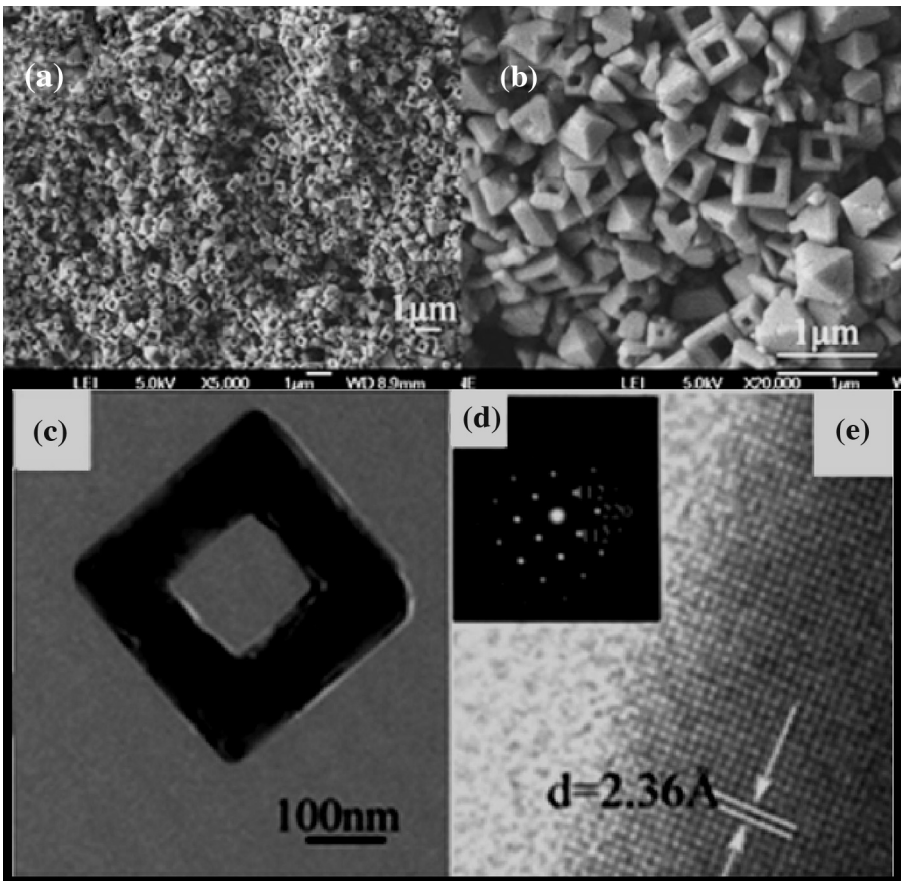

Fig. 13. FE-SEM, TEM and HR-TEM images of the as-synthesized birnessite-type manganese oxide nanobelts by the hydrothermally route using a KOH–Mn^{2+}–MnO_4^- system [123].

bonding between Mn^{VII} and O^{-2}, leading to a noticeable modification of the evolution of Mn-oxide nanostructures with various morphologies. Therefore, there is great interest in Mn-oxides, especially in nanosized forms, for both rudimentary and practical reasons. The preparation of Mn-oxide nanostructures using $KMnO_4$ is an open research topic regarding their role in materials science in the formation of new structures and morphologies and is expected to become increasingly significant in crystal growth theory.

3.5. Birnessite and cryptomelane

Birnessite is a common component of manganese nodules, which was found to be effective in oxidation, reduction, decomposition and demetallation reactions due to its relatively high surface area and transition metal oxide content. The use of birnessite-type MnO_2 has become popular due to its layered structure, which is beneficial for the intercalation and deintercalation of H^+ or alkali metal cations and shows promising properties for enhancing the special capacitance [120]. Since the early report of layer-structured brown birnessite with microscale structures by McKenzie [121], many of the published methods provide only brief descriptions, and duplication of these methods is difficult because of the lack of detail; seemingly minor variations in conditions or starting materials can influence the results. Thin films of birnessite are fabricated on indium tin oxide-coated polyethylene terephthalate substrates by chemical bath deposition technology from an alkaline $KMnO_4$ aqueous solution at room temperature [122]. Fig. 13 shows the delamination of manganese oxide nanobelts with the birnessite-type layered structure having a length of several tens of micrometres, a width of hundreds of nanometres, and a thickness of 15 nm. These nanobelts were synthesized by hydrothermally treating a $KMnO_4$–$MnCl_2$ mixture in a highly concentrated KOH aqueous solution. The nanobelt growth was controlled by the KOH concentration and the molar ratio of Mn^{2+}/MnO_4^- in the starting reaction mixture. The monoclinic K-birnessite nanobelts were converted

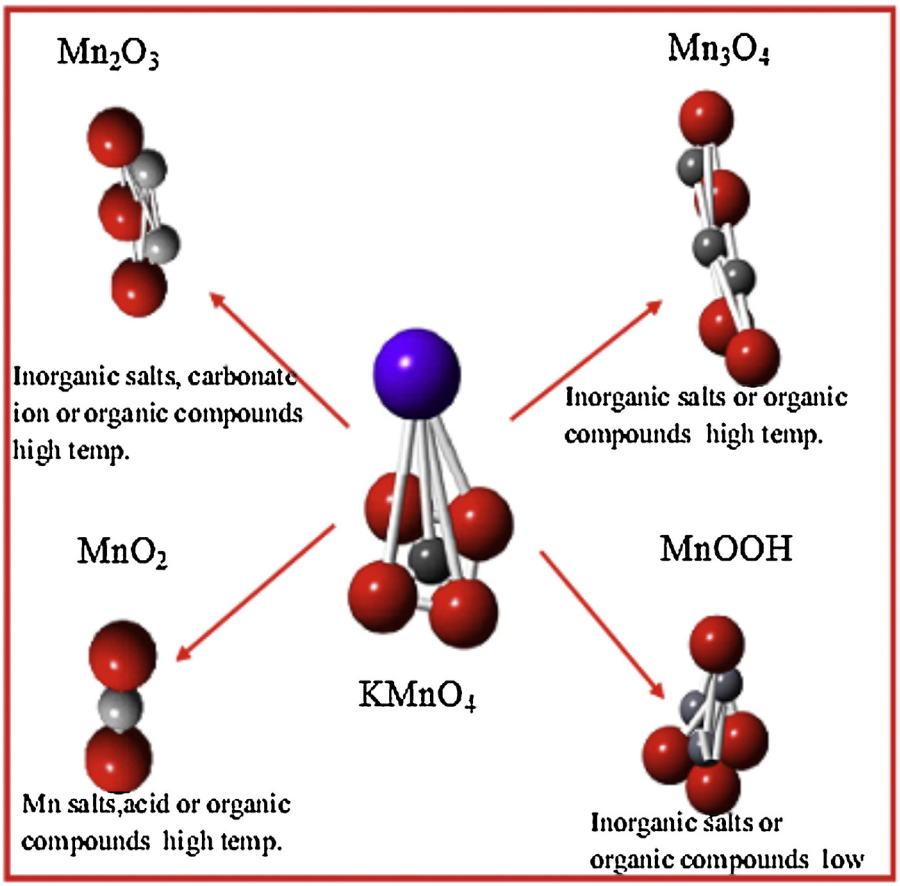

Fig. 14. Schematic illustration of reduction permanganate kinetics by many organic substrates.

to hexagonal H-birnessite nanobelts, ascribed to the noticeably decreased amount of Mn^{3+}, which should release the steric strain arising from Jahn–Teller distortion [123]. Monodisperse manganese oxide honeycombs and hollow nanospheres were reported by the decomposition of $KMnO_4$ in oleic acid using an ultrasonic method [124]. In our previous work, the flower-like birnessite-type manganese oxide hierarchical architectures were achieved by reducing $KMnO_4$ with a sodium fluorite solution in sulfuric acid medium [125]. Recently, the effect of Hoffmeister anions, such as Cl^-, $SO_4{}^{2-}$, and $ClO_4{}^-$, on the structure and morphology of birnessite and cryptomelane-type manganese dioxide nanostructures was studied [126].

Because it is constructed of double chains of edge-sharing MnO_6 octahedra forming square cross-section tunnels with two MnO_6 on each side, cryptomelane-type manganese oxides are of considerable interest, and they have been widely used as catalysts, chemical sensors, ion-exchangers, solid ionic conductors and battery materials [127]. Until now, many structures of OMS-2 were prepared by the redox precipitation technique. Among them, one-dimensional structures such as nanowires and nanofibers were prepared by reacting $KMnO_4$ with $MnSO_4$ under hydrothermal conditions [128,129]. The growth stage proceeds by the solution route or by oriented attachment, depending on the growth direction. In the last few years, the synthesis metals incorporated in OMS-2 nanocrystals have attracted increasing research interest in scientific studies and in technological development. Manganese oxide nanocrystals can be isomorphously doped with a number of different transition metals by reducing $KMnO_4$. Lee et al. [130] employed $CoSO_4$ and ammonium persulfate solutions as reducer materials to synthesize $K_xMn_{1-y}Co_yO_{2-\delta}$ nanowires

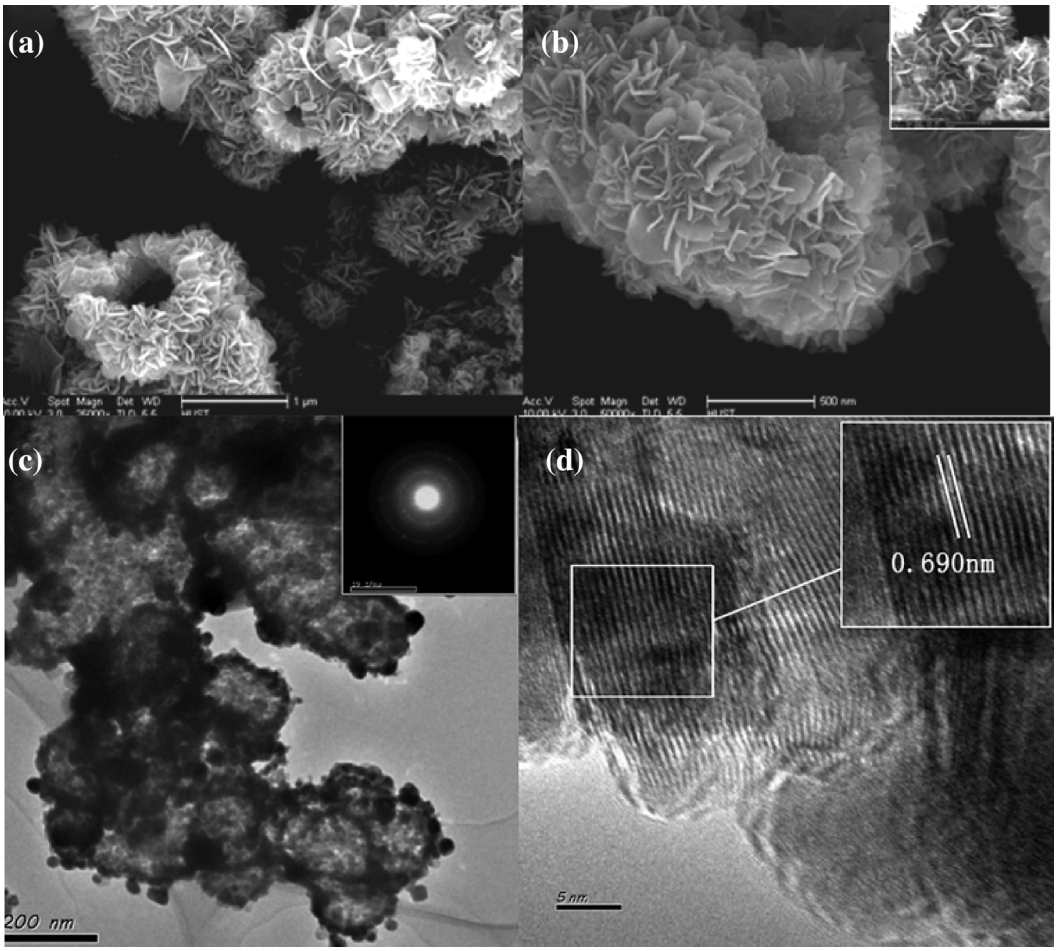

Fig. 15. SEM, TEM and HR-TEM images of a $K_xCo_yMn_{8-y}O_{16}$ microsphere prepared by the hydrothermal method with a Co/Mn molar ratio of 1:1 at 140 °C for 14 h [131].

and 3D hierarchically assembled microspheres under hydrothermal conditions. The dimensions were easily controlled by cation composition, alternating the reactant ratio and reaction temperature. In our previous work, cobalt acetate directly formed an urchin-like $K_xCo_yMn_{8-y}O_{16}$ hollow spheres assembly of nanoplate building blocks [131]. The hollow sphere of $K_xCo_yMn_{8-y}O_{16}$ has an average diameter of 1.2 μm, a shell thickness of 150 nm and a diameter of the hollow cavity of 350 nm; it is polycrystalline, with a lattice spacing of 0.686 nm, and {1 1 0} fringes of hollow structures were observed from the transference of {1 0 1} $KMnO_4$ as followed by Ostwald ripening and dissolution re-crystallization mechanisms as the suggested processes (Fig. 15). The effects of cobalt ions on the physicochemical properties were examined for the catalytic removal of toxic material from water, degradation of dyes and oxidation of organic materials. However, the mechanism for the positive effect of Co substitution is currently unclear due to the strong oxidation power of Co^{3+}/Co^{4} ions compared with Mn^{3+}/Mn^{4+}ions [132]. Manganese oxide octahedral molecular sieve (OMS) materials with tunnel structures have recently attracted interest because of their small particle sizes and larger surface areas, which can improve the performance of manganese oxide materials in applications such as catalysts and battery materials [133]. Iron-doped cryptomelane obtained by the thermal transformation of iron-doped birnessite have exploited the catalytic properties [134].

4. Conclusions

This review provides a comprehensive introduction of various preparation methods for nanostructured manganese oxyhydroxides, manganese oxides and metal-incorporated manganese oxides, including our precursor $KMnO_4$ as the raw material. The formation mechanisms of these nanomaterials are proposed for a better understanding and utilization of the role of this material. Therefore, many studies must be performed to find general, economic and effective methods of fabricating manganese oxide nanomaterials for industrial applications. In addition to its use in preparations, this material also has applications in catalysis, medicine and electrochemical areas.

Acknowledgments

The researcher would like to thank the Faculty of Science and Education, Department of Chemistry, Taif University for partially supporting this research and allowing sufficient time to write this article (Project 1-435-2998).

References

[1] Z. Chen, Z. Jiao, D. Pan, Z. Li, M. Wu, C.H. Shek, C.M.L. Wu, J.K.L. Lai, Recent advances in manganese oxide nanocrystals: fabrication, characterization, and microstructure, Chem. Rev. 112 (2012) 3833–3855.
[2] A.J. Zarur, J.Y. Ying, Reverse microemulsion synthesis of nanostructured complex oxides for catalytic combustion, Nature 403 (2000) 65–67.
[3] C. Burda, X. Chen, R. Narayanan, M.A. El-Sayed, Chemistry and properties of nanocrystals of different shapes, Chem. Rev. 105 (2005) 1025–1102.
[4] L. Wang, J.S. Yin, W.D. Mo, Z.J. Zhang, In-situ analysis of valence conversion in transition metal oxides using electron energy loss spectroscopy, J. Phys. Chem. B 101 (1997) 6793–6798.
[5] R.E. Newnham, G.R. Ruschau, Smart electroceramics, J. Am. Ceram. Soc. 74 (1991) 463–480.
[6] C.B. Murray, D.J. Norris, M.G. Bawendi, Synthesis and characterization of nearly monodisperse CdE (E = sulfur, selenium, tellurium) semiconductor nanocrystallites, J. Am. Chem. Soc. 115 (1993) 8706–8715.
[7] D.O. Dabbouusi, J.R. Viejo, F.V. Mikulec, J.R. Heine, H. Mattoussi, R. Ober, K.F. Jensen, M.G. Bawendi, J. Phys. Chem. B 101 (1997) 9463–9475.
[8] K. Manzoor, S.R. Vadera, N. Kumar, T.R. Kutty, Synthesis and photoluminescent properties of ZnS nanocrystals doped with copper and halogen, J. Mater. Chem. Phys. 82 (2003) 718–725.
[9] M.Y. Masoomi, A. Morsali, Applications of metal–organic coordination polymers as precursors for preparation of nanomaterials, Coord. Chem. Rev. 256 (2012) 2921–2943.
[10] C.N.R. Rao, A. Govindaraj, S.R.C. Vivekchand, Inorganic nanomaterials: current status and future prospects, Annu. Rep. Sect. A: Inorg. Chem. 102 (2006) 20–45.
[11] C.N.R. Rao, S.R.C. Vivekchand, K. Biswasa, A. Govindaraj, Synthesis of inorganic nanomaterials, Dalton Trans. 34 (2007) 3728–3749.
[12] M.E. Weeks, H.M. Leicester, Discovery of the Elements, 7th ed., Journal of Chemical Education, Easton, PA, 1968, pp. 351–382.
[13] C.M. Kao, K.D. Huang, J.Y. Wang, T.Y. Chen, H.Y. Chien, Application of potassium permanganate as an oxidant for in situ oxidation of trichloroethylene-contaminated groundwater: a laboratory and kinetics study, J. Hazard. Mater. 153 (2008) 919–927.
[14] R.H. Waldemer, P.G. Tratnyek, Kinetics of contaminant degradation by permanganate, Environ. Sci. Technol. 40 (2006) 1055–1061.
[15] M.A. Urynowicz, In-situ chemical oxidation with permanganate: assessing the competitive interactions between target and nontarget compounds, Soil Sediment Contam. 17 (2008) 53–62.
[16] J.G. Freitas, B. Fletcher, R. Aravena, J.F. Baker, Methane production and isotopic fingering in ethanol fuel contaminated sites, Groundwater 48 (2010) 844–857.
[17] M.G. Mahmoodlu, N. Hartog, S.M. Hassanizadeh, A. Raoof, Oxidation of volatile organic vapours in air by solid potassium permanganate, Chemosphere 91 (2013) 1534–1538.

[18] X. Xu, H. Li, W. Wang, J. Gu, Decolorization of dyes and textile wastewater by potassium permanganate, Chemosphere 59 (2005) 893–898.
[19] Y.Y. Eugene, F.W. Schwartz, Oxidative degradation and kinetics of chlorinated ethylenes by potassium permanganate, J. Contam. Hydrol. 37 (1999) 343–365.
[20] J.H. Damm, C. Hardacre, R.M. Kalin, K.P. Walsh, Kinetics of the oxidation of methyl-tert-butyl ether (MTBE) by potassium permanganate, Water Res. 36 (2002) 3638–3646.
[21] E. Rodrıguez, M.E. Majado, J. Meriluoto, J.L. Acero, Oxidation of microcystins by permanganate: reaction kinetics and implications for water treatment, Water Res. 41 (2007) 102–110.
[22] J. Ma, N. Graham, G. Li, Effect of permanganate preoxidation in enhancing the coagulation of surface water – laboratory case studies, J. Water Supply: Res. Technol. – Aqua 46 (1997) 1–10.
[23] A. Shaabani, P. Mirzaei, S. Naderi, D.G. Lee, Green oxidations. The use of potassium permanganate supported on manganese dioxide, Tetrahedron 60 (2004) 11415–11420.
[24] B.A. Lay, Application of potassium permanganate in fish culture, Trans. Am. Fish. Soc. 100 (1971) 813–815.
[25] A. Aleboyeh, M.E. Olya, H. Aleboyeh, Oxidative treatment of azo dyes in aqueous solution by potassium permanganate, J. Hazard. Mater. 162 (2009) 1530–1535.
[26] S. Dash, S. Patel, B.K. Mishr, Oxidation of styrylpyridinium dyes by permanganate ion, Tetrahedron 65 (2009) 707–739.
[27] F.W. Schwartz, Permanganate treatment of DNAPLs in reactive barriers and source zone flooding schemes. Final report, U.S. Department of Energy, 2000.
[28] Y. Seol, F.W. Schwartz, S. Lee, Oxidation of binary DNAPL mixtures using potassium permanganate with a phase transfer catalyst, Groundw. Monit. Remediat. 21 (2001) 124–132.
[29] F. Davar, F. Mohandes, M.S. Niasari, Synthesis and characterization manganese oxide nanobundles from decomposition of manganese oxalate, Inorg. Chim. Acta 362 (2009) 3663–3668.
[30] C.M. Cellier, V. Vromman, V. Ruaux, E.M. Gaigneaux, Sulfation mechanism and catalytic behavior of manganese oxide in the oxidation of methanethiol, J. Phys. Chem. B 108 (2004) 9989–10001.
[31] H.M. Chen, J.H. He, Facile synthesis of monodisperse manganese oxide nanostructures and their application in water, J. Phys. Chem. C 112 (2008) 17540–17545.
[32] O. Giraldo, S.L. Brock, W.S. Willis, M. Marquez, S.L. Suib, Manganese oxide thin films with fast ion-exchange properties, J. Am. Chem. Soc. 122 (2000) 9330–9331.
[33] X.H. Tang, Z.H. Liu, C.X. Zhang, Z.P. Yang, Z.L. Wang, Synthesis and capacitive property of hierarchical hollow manganese oxide nanospheres with large specific surface area, J. Power Sources 193 (2009) 939–943.
[34] C.Z. Yuan, B. Gao, L.H. Su, X.G. Zhang, Interface synthesis of mesoporous MnO_2 and its electrochemical capacitive behaviors, J. Colloid Interface Sci. 322 (2008) 545–550.
[35] R.Z. Ma, Y. Bando, L.Q. Zhang, T. Sasaki, Layered MnO_2 nanobelts: hydrothermal synthesis and the electrochemical measurements, Adv. Mater. 16 (2004) 918–922.
[36] W. Xiao, J.S. Chen, Q. Lu, X.W. Lou, Porous spheres assembled from polythiophene (PTh)-coated ultrathin MnO_2 nanosheets with enhanced lithium storage capabilities, J. Phys. Chem. C 114 (2010) 12048–12051.
[37] D.W. Liu, B.B. Garcia, Q.F. Zhang, Q. Guo, Y.H. Zhang, S. Sepehri, G.Z. Cao, Mesoporous hydrous manganese dioxide nanowall arrays with large lithium ion energy storage capacities, Adv. Funct. Mater. 19 (2009) 1015–1021.
[38] F.Y. Cheng, J.Z. Zhao, W. Song, C.S. Li, H. Ma, J. Chen, P.W. Shen, Facile controlled synthesis of MnO_2 nanostructures of novel shapes and their application in batteries, Inorg. Chem. 45 (2006) 2038–2044.
[39] G.L. Wang, B. Tang, L.H. Zhuo, J.C. Ge, M. Xue, Facile and selected-control synthesis of beta-MnO_2 nanorods and their magnetic properties, Eur. J. Inorg. Chem. 11 (2006) 2313–2317.
[40] H.T. Zhu, J. Luo, H.X. Yang, J.K. Liang, G.H. Rao, J.B. Li, Z.M. Du, Birnessite-type MnO_2 nanowalls and their magnetic properties, J. Phys. Chem. C 112 (2008) 17089–17094.
[41] S. Zhang, S. Long, W. Guan, Q. Liu, Q. Wang, M. Liu, Resistive switching characteristics of MnO_x-based ReRAM, J. Phys. D: Appl. Phys. 42 (2009) 055112–055116.
[42] W. Meggison, H. Hollinworth, Using potassium permanganate for wound cleansing, J. Wound Care 3 (4) (1994) 194.
[43] C.M. Quartey-Papafio, Importance of distinguishing between cellulitis and varicose eczema of the leg, Br. Med. J. 318 (1999) 1672–1673.
[44] S. Baron, C. Moss, Caustic burn caused by potassium permanganate, Arch. Dis. Child. 88 (2003) 96.
[45] S.J. You, Q.L. Zhao, J.N. Zhang, J.Q. Jiang, S.Q. Zhao, A microbial fuel cell using permanganate as the cathodic electron acceptor, J. Power Sources 162 (2006) 1409–1415.
[46] H. Liu, B.E. Logan, Electricity generation using an air-cathode single chamber microbial fuel cell in the presence and absence of a proton exchange membrane, Environ. Sci. Technol. 38 (2004) 4040–4046.
[47] I. Popa, A. Dragos, I. Taranu, M. Stefanut, C. Vaszilcsin, D.L. Buzatu, Electrochemical synthesis of the pyrazine-2,3-dicarboxylic acid. Electrochemical kinetic studies on platinum electrode, Chem. Bull. 52 (2007) 99–103.
[48] A. Hamdy, H.M. Hussien, Deposition, characterization and electrochemical properties of permanganate-based coating treatments over ZE41 Mg–Zn–rare earth alloy, Int. J. Electrochem. Sci. 8 (2013) 11386–11402.
[49] J.D. Hanawalt, H.W. Rinn, L.K. Frevel, Chemical analysis by X-ray diffraction, Ind. Eng. Chem. Anal. Ed. 10 (1938) 475–512.
[50] G.J. Palenik, Crystal structure of potassium permanganate, Inorg. Chem. 6 (1967) 503–507.
[51] R.C.L. Mooney, The crystal structure of potassium permanganate, Phys. Rev. 37 (1931) 1306–1310.
[52] D. Marabello, R. Bianchi, G. Gervasio, F. Cargnoni, An experimental (120 K) and theoretical electron density study of $KMnO_4$ and $KClO_4$, Acta Crystallogr. Sect. A 60 (2004) 494–501.
[53] Y. Zhang, Y. Liu, F. Guo, Y. Hu, X. Liu, Y. Qian, Single-crystal growth of MnOOH and beta-MnO_2 microrods at lower temperatures, Solid State Commun. 134 (2005) 523–527.
[54] G. Xi, Y. Peng, Y. Zhu, L. Xu, W. Zhang, W. Yu, Y. Qian, Preparation of β-MnO_2 nanorods through a γ-MnOOH precursor route, Mater. Res. Bull. 39 (2004) 1641–1648.
[55] Z. Li, H. Bao, X. Miao, X. Chen, A facile route to growth of γ-MnOOH nanorods and electrochemical capacitance properties, J. Colloid Interface Sci. 357 (2011) 286–291.
[56] T. Gao, F. Krumeich, R. Nesper, H. Fjellva, P. Norby, Microstructures, surface properties, and topotactic transitions of manganite nanorods, Inorg. Chem. 48 (2009) 6242–6250.
[57] K.A.M. Ahmed, H. Peng, K. Wu, K. Huang, Hydrothermal preparation of nanostructured manganese oxides (MnO_x) and their electrochemical and photocatalytic properties, Chem. Eng. J. 172 (2011) 531–539.

[58] Y. Li, H. Tan, O. Lebedev, J. Verbeeck, E. Biermans, G.V. Tendeloo, B.L. Su, Insight into the growth of multiple branched MnOOH nanorods, Cryst. Growth Des. 10 (2010) 2969–2976.
[59] L. Zhang, X. Zhang, Z. Wang, J. Xu, D. Xua, L. Wang, High aspect ratio γ-MnOOH nanowires for high performance rechargeable nonaqueous lithium-oxygen batteries, Chem. Commun. 48 (2012) 759–760.
[60] K.A.M. Ahmed, H.A. Abbood, K. Huang, Hydrothermal synthesis of Mn(OH)O nanowires and their thermal conversion to (1D)-manganese oxides nanostructures, J. Cryst. Growth 358 (2012) 33–37.
[61] D. Portehault, S. Cassaignon, E. Baudrin, J.-P. Jolivet, Evolution of nanostructured manganese (oxyhydr)oxides in water through MnO_4^- reduction, Cryst. Growth Des. 10 (2010) 2168–2173.
[62] C. Xia, C. Xiaolan, W. Ning, Selective sensing of dopamine at MnOOH nanobelt modified electrode, Sens. Actuators B 160 (2011) 771–776.
[63] Y.-T. Wu, C.-C. Hu, Aspect ratio controlled growth of MnOOH in mixtures of Mn_3O_4 and MnOOH single crystals for supercapacitors, Electrochem. Solid State Lett. 8 (2005) A240–A244.
[64] M.S. El-Deab, Electrocatalytic oxidation of methanol at γ-MnOOH nanorods modified Pt electrodes, Int. J. Electrochem. Sci. 4 (2009) 1329–1338.
[65] Z.Y. Yuan, T.Z. Ren, G.H. Du, B.L. Su, Facile preparation of single-crystalline nanowires of γ-MnOOH and β-MnO_2, Appl. Phys. A 80 (2005) 743–747.
[66] Z. Zhang, J. Mu, Hydrothermal synthesis of γ-MnOOH nanowires and α-MnO_2 sea urchin-like clusters, Solid State Commun. 141 (2007) 427–430.
[67] Q. Tang, X. Gong, C. Wu, Y. Chen, A. Borgna, Y. Yang, Insights into the nature of alumina-supported MnOOH and its catalytic performance in the aerobic oxidation of benzyl alcohol, Catal. Commun. 10 (2009) 1122–1126.
[68] L. Qi, Colloidal chemical approaches to inorganic micro- and nanostructures with controlled morphologies and patterns, Coord. Chem. Rev. 254 (2010) 1054–1071.
[69] Y. Chabre, J. Pannetier, Structural and electrochemical properties of the proton gamma MnO_2 system, Prog. Solid State Chem. 23 (1995) 1–130.
[70] L. Espinal, S.L. Suib, J.F. Rusling, Electrochemical catalysis of styrene epoxidation with films of MnO_2 nanoparticles and H_2O_2, J. Am. Chem. Soc. 126 (2004) 7676–7682.
[71] R. Chitrakar, H. Kanoh, Y.S. Kim, Y. Miyai, K. Ooi, J. Solid State Chem. 160 (2001) 69–76.
[72] A.R. Armstrong, P.G. Bruce, Synthesis of layered $LiMnO_2$ as an electrode for rechargeable lithium batteries, Nature 381 (1996) 499–500.
[73] B. Ammundsen, J. Paulsen, Novel lithium-ion cathode materials based on layered manganese oxides, Adv. Mater. 13 (2001) 943–956.
[74] M. Winter, R.J. Brodd, What are batteries, fuel cells, and supercapacitors? Chem. Rev. 104 (2004) 4245–4269.
[75] L.C. Zhang, Z.H. Liu, X.H. Tang, J.F. Wang, K. Ooi, Synthesis and characterization of β-MnO_2 single crystals with novel tetragonous morphology, Mater. Res. Bull. 42 (2007) 1432–1439.
[76] Q. Feng, H. Kanoh, K. Ooi, Manganese oxide porous crystals, J. Mater. Chem. 9 (1999) 319–334.
[77] F. Schurz, J.M. Bauchert, T. Merker, T. Schleid, H. Hasse, R. Glaser, Octahedral molecular sieves of the type K-OMS-2 with different particle sizes and morphologies: impact on the catalytic properties in the aerobic partial oxidation of benzyl alcohol, Appl. Catal. A: Gen. 355 (2009) 42–49.
[78] B. Ming, J. Li, F. Kang, G. Pang, Y. Zhang, L. Chen, J. Xu, X. Wang, Microwave-hydrothermal synthesis of birnessite-type MnO_2 nanospheres as supercapacitor electrode materials, J. Power Sources 198 (2012) 428–431.
[79] M.A. Cheney, S.W. Joo, A. Banerjee, B.-K. Min, Efficient production of ultrapure manganese oxides via electrodeposition, J. Colloid Interface Sci. 379 (2012) 141–143.
[80] Z. Song, W. Liu, M. Zhao, Y. Zhang, G. Liu, C. Yu, J. Qi, A facile template-free synthesis of a-MnO_2 nanorods for supercapacitor, J. Alloys Compd. 560 (2013) 151–155.
[81] X. Fu, J. Feng, H. Wang, K.M. Ng, Morphological and structural evolution of α-MnO_2 nanorods synthesized via an aqueous route through MnO_4^-/Mn^{2+} reaction, J. Solid State Chem. 183 (2010) 883–889.
[82] Y. Li, H. Xie, J. Wang, L. Chen, Preparation and electrochemical performances of α-MnO_2 nanorod for supercapacitor, Mater. Lett. 65 (2011) 403–405.
[83] V. Subramanian, H. Zhu, R. Vajtai, P.M. Ajayan, B. Wei, Hydrothermal synthesis and pseudocapacitance properties of MnO_2 nanostructures, J. Phys. Chem. B 109 (2005) 20207–20214.
[84] Y. Wu, S. Li, Y. Cao, S. Xing, Z. Ma, Y. Gao, Facile synthesis of mesoporous α-MnO_2 nanorod with three-dimensional frameworks and its enhanced catalytic activity for VOCs removal, Mater. Lett. 97 (2013) 1–3.
[85] M. Toupin, T. Brousse, D. Belanger, Influence of microstructure on the charge storage properties of chemically synthesized manganese dioxide, Chem. Mater. 14 (2002) 3946–3952.
[86] N. Tang, X. Tian, C. Yang, Z. Pi, Q. Han, Facile synthesis of α-MnO_2 nanorods for high-performance alkaline batteries, J. Phys. Chem. Solids 71 (2010) 258–262.
[87] M. Xu, L. Kong, W. Zhou, H. Li, Hydrothermal synthesis and pseudocapacitance properties of α-MnO_2 hollow spheres and hollow urchins, J. Phys. Chem. C 111 (2007) 19141–19147.
[88] Q. Zhang, Z. Xiao, X. Feng, W. Tan, G. Qiu, F. Liu, α-MnO_2 nanowires transformed from precursor δ-MnO_2 by refluxing under ambient pressure: the key role of pH and growth mechanism, Mater. Chem. Phys. 125 (2011) 678–685.
[89] J. Luo, H.T. Zhu, H.M. Fan, J.K. Liang, H.L. Shi, G.H. Rao, J.B. Li, Z.M. Du, Z.X. Shen, Synthesis of single-crystal tetragonal α-MnO_2 nanotubes, J. Phys. Chem. C 112 (2008) 12594–12598.
[90] K. Chen, Y.D. Noh, K. Li, S. Komarneni, D. Xue, Microwave-hydrothermal crystallization of polymorphic MnO_2 for electrochemical energy storage, J. Phys. Chem. C 117 (2013) 10770–10779.
[91] T.-D. Dang, A.N. Banerjee, S.W. Joo, B.-K. Min, Synthesis of amorphous and crystalline hollow manganese oxide nanotubes with highly porous walls using carbon nanotube templates and enhanced catalytic activity, Ind. Eng. Chem. Res. 53 (2014) 9743–9753.
[92] Z. Yang, C. Zhou, W. Zhang, H. Li, M. Chen, β-MnO_2 nanorods: a new and efficient catalyst for isoamyl acetate synthesis, Colloids Surf. A: Physicochem. Eng. Asp. 356 (2010) 134–139.
[93] C. Wei, C. Xu, B. Li, D. Nan, J. Ma, F. Kang, Formation and conversion mechanisms between single-crystal gamma-MnOOH and manganese oxides, Mater. Res. Bull. 47 (2012) 1740–1746.
[94] D. Yan, P.X. Yan, G.H. Yue, J.Z. Liu, J.B. Chang, Q. Yang, D.M. Qu, Z.R. Geng, J.T. Chen, G.A. Zhang, R.F. Zhuo, Self-assembled flower-like hierarchical spheres and nanobelts of manganese oxide by hydrothermal method and

morphology control of them, Chem. Phys. Lett. 440 (2007) 134–138.
[95] J. Fei, Y. Cui, X. Yan, W. Qi, Y. Yang, K. Wang, Q. He, J. Li, Controlled preparation of MnO_2 hierarchical hollow nanostructures and their application in water treatment, Adv. Mater. 20 (2008) 452–456.
[96] Y. Gu, J. Cai, M. He, L. Kang, Z. Lei, Z.-H.i. Liu, Preparation and capacitance behavior of manganese oxide hollow structures with different morphologies via template-engaged redox etching, J. Power Sources 239 (2013) 347–355.
[97] X. He, M. Yang, P. Ni, Y. Li, Z.-H. Liu, Rapid synthesis of hollow structured MnO_2 microspheres and their capacitance, Colloids Surf. A: Physicochem. Eng. Asp. 363 (2010) 64–70.
[98] T.D. Dang, A.N. Banerjee, M.A. Cheney, S. Qian, S.W. Joo, B.K. Min, Bio-silica coated with amorphous manganese oxide as an efficient catalyst for rapid degradation of organic pollutant, Colloids Surf. B: Biointerfaces 106 (2013) 151–157.
[99] Y.P. Liu, Y.T. Qian, Y.H. Zhang, M.W. Zhang, Z.Y. Chen, L. Yang, C.S. Wang, Z.W. Chen, Preparation of nanocrystalline manganic oxide Mn_2O_3 powders by use of γ-ray radiation, Mater. Lett. 28 (1996) 357–359.
[100] Z.-W. Chen, S.-Y. Zhang, S. Tan, J. Wang, S.Z. Jin, Different aspects of the microstructure of nanometer-sized Mn_2O_3, Mater. Res. Bull. 34 (1999) 1583–1587.
[101] S.D. Skapin, Š. Kunej, D. Suvorov, Phase relations and electrical properties in the pseudo-ternary La_2O_3–TiO_2–Mn_2O_3 system in air, J. Eur. Ceram. Soc. 28 (2008) 3119–3124.
[102] M. Salavati-Niasari, F. Mohandes, F. Davar, K. Saberyan, Fabrication of chain-like Mn_2O_3 nanostructures via thermal decomposition of manganese phthalate coordination polymers, Appl. Surf. Sci. 256 (2009) 1476–1480.
[103] Z. Gui, R. Fan, X.H. Chen, Y.C. Wu, A simple direct preparation of nanocrystalline gamma-Mn_2O_3 at ambient temperature, Inorg. Chem. Commun. 4 (2001) 294–296.
[104] P.K. Sharma, M.S. Whittingham, The role of tetraethyl ammonium hydroxide on the phase determination and electrical properties of gamma-MnOOH synthesized by hydrothermal, Mater. Lett. 48 (2001) 319–323.
[105] Y.P. Liu, Y. Qian, Y. Zhang, M. Zhang, Z. Chen, L. Yang, C. Wang, Z. Chen, Preparation of nanocrystalline manganic oxide Mn_2O_3 powders by use of γ-ray radiation, Mater. Lett. 28 (1996) 357–359.
[106] J. Cao, Y. Zhu, K. Bao, L. Shi, S. Liu, Y. Qian, Microscale Mn_2O_3 hollow structures: sphere, cube, ellipsoid, dumbbell, and their phenol adsorption properties, J. Phys. Chem. C 113 (2009) 17755–17760.
[107] J. Cao, Y. Zhu, L. Shi, L. Zhu, K. Bao, S. Liu, Y. Qian, Double-shelled Mn_2O_3 hollow spheres and their application in water treatment, Eur. J. Inorg. Chem. (2010) 1172–1176.
[108] Y.C. Chen, Y.G. Zhang, Q.Z. Yao, G.T. Zhou, S.Q. Fu, H. Fan, Formation of α-Mn_2O_3 nanorods via a hydrothermal-assisted cleavage-decomposition mechanism, J. Solid State Chem. 180 (2007) 1218–1223.
[109] T.-D. Dang, A.N. Banerjee, S.W. Joo, B.-K. Min, Effect of potassium ions on the formation of crystalline manganese oxide nanorods via acidic reduction of potassium permanganate, Ind. Eng. Chem. Res. 52 (2013) 14154–14159.
[110] F.A. Al Sagheer, M.A. Hasan, L. Pasupulety, M.I. Zaki, Low-temperature synthesis of hausmannite Mn_3O_4, J. Mater. Sci. Lett. 18 (1999) 209–211.
[111] W. Zhang, C. Wang, Y.T. Qian, Low temperature synthesis of nanocrystalline Mn_3O_4 by a solvothermal method, Solid State Ionics 117 (1999) 331–335.
[112] Y.C. Zhang, T. Qiao, X.Y. Hu, Preparation of Mn_3O_4 nanocrystallites by low-temperature temperature solvothermal treatment of γ-MnOOH nanowires, J. Solid State Chem. 177 (2004) 4093–4097.
[113] J. Du, Y. Gao, L. Chai, G. Zou, Y. Li, Y. Qian, Hausmannite Mn_3O_4 nanorods: synthesis, characterization and magnetic properties, Nanotechnology 17 (2006) 4923–4928.
[114] B. Yang, H. Hu, C. Li, X. Yang, Q. Li, Y. Qian, One-step route to single-crystal γ-Mn_3O_4 nanorods in alcohol–water system, Chem. Lett. 33 (2004) 804–805.
[115] Y. Z-Heng, Z. Chen-xu, S. Xinmin, Z. Wei-Xin, Z. Na, Synthesis of various nanostructured manganese oxides via facile hydrothermal reaction, Chin. J. Inorg. Chem. 24 (2008) 1695–1700.
[116] P. Gibot, L. Laffont, Hydrophilic and hydrophobic nanosized Mn_3O_4 particles, J. Solid State Chem. 180 (2007) 695–701.
[117] J.W. Lee, A.S. Hall, J.-D. Kim, T.E. Mallouk, A facile and template-free hydrothermal synthesis of Mn_3O_4 nanorods on graphene sheets for supercapacitor electrodes with long cycle stability, Chem. Mater. 24 (2012) 1158–1164.
[118] J. Yin, F. Gao, Y. Wu, J. Wang, Q. Lu, Synthesis of Mn_3O_4 octahedrons and other manganese-based nanostructures through a simple and green route, Cryst. Eng. Commun. 12 (2010) 3401–3403.
[119] Y. Liu, Z.-F. Gao, Q. Sun, Y.-P. Zeng, Template-assisted synthesis of single-crystalline Mn_3O_4 nanoframes and hollow octahedra, Solid State Sci. 14 (2012) 1462–1466.
[120] S. Ching, D.J. Petrovay, M.L. Jorgensen, Sol–gel synthesis of layered birnessite-type manganese oxides, Inorg. Chem. 36 (1997) 883–890.
[121] R.M. McKenzie, The synthesis of birnessite, cryptomelane, and some other oxides and hydroxides of manganese, Mineral. Mag. 38 (1971) 493–502.
[122] Y. Hu, H. Zhu, J. Wang, Z. Chen, Synthesis of layered birnessite-type manganese oxide thin films on plastic substrates by chemical bath deposition for flexible transparent supercapacitors, J. Alloys Compd. 509 (2011) 10234–10240.
[123] Z. Liu, R. Ma, Y. Ebina, K. Takada, T. Sasaki, Synthesis and delamination of layered manganese oxide nanobelts, Chem. Mater. 19 (2007) 6504–6512.
[124] H. Chen, J. He, C. Zhang, H. He, Self-assembly of novel mesoporous manganese oxide nanostructures and their application in oxidative decomposition of formaldehyde, J. Phys. Chem. C 111 (2007) 18033–18038.
[125] K.A.M. Ahmed, K. Huang, Rapid synthesis of novel flowerlike $K_{0.46}Mn_2O_4(H_2O)_{1.4}$ hierarchical architectures and their catalytic degradation of formaldehyde in aqueous solution, Solid State Sci. 30 (2014) 11–16.
[126] M.A. Cheney, R. Jose, A. Banerjee, P.K. Bhowmik, S. Qian, J.M. Okoh, Synthesis and characterization of birnessite and cryptomelane nanostructures in presence of Hoffmeister anions, J. Nanomater. (2009), http://dx.doi.org/10.1155/2009/940462.
[127] Y. Lin, X. Cui, L. Li, Low-potential amperometric determination of hydrogen peroxide with a carbon paste electrode modified with nanostructured cryptomelane-type manganese oxides, Electrochem. Commun. 7 (2005) 166–172.
[128] D. Portehault, S. Cassaignon, E. Baudrin, J.-P. Jolivet, Morphology control of cryptomelane type MnO_2 nanowires by soft

chemistry. Growth mechanisms in aqueous medium, Chem. Mater. 19 (2007) 5410–5417.

[129] T. Gao, M. Glerup, F. Krumeich, R. Nesper, H. Fjellvåg, P. Norby, Microstructures and spectroscopic properties of cryptomelane-type manganese dioxide nanofibers, J. Phys. Chem. C 112 (2008) 13134–13140.

[130] S.H. Lee, T.W. Kim, D.H. Park, J.-H. Choy, S.J. Hwang, Single-step synthesis, characterization, and application of nanostructured $K_xMn_{1-y}CoyO_{2-\delta}$ with controllable chemical compositions and crystal structures, Chem. Mater. 19 (2007) 5010–5017.

[131] K.A.M. Ahmed, B. Li, B. Tan, K. Huang, Urchin-like cobalt incorporated manganese oxide OMS-2 hollow spheres: synthesis, characterization and catalytic degradation of RhB dye, Solid State Sci. 15 (2013) 66–72.

[132] H. Yin, X. Feng, G. Qiu, W. Tan, F. Liu, Lead adsorption and arsenite oxidation by cobalt doped birnessite, J. Hazard. Mater. 188 (2011) 341–349.

[133] J. Liu, J. Cai, Y. Son, Q. Gao, S.L. Suib, M. Aindow, Magnesium manganese oxide nanoribbons: synthesis, characterization, and catalytic application, J. Phys. Chem. B 106 (2002) 9761–9768.

[134] J. Cai, J. Liu, W.S. Willis, S.L. Suib, Framework doping of iron in tunnel structure cryptomelane, Chem. Mater. 13 (2001) 2413–2422.